Microbial Ecology
https://doi.org/10.1007/s00248-019-01322-w

MICROBIOLOGY OF AQUATIC SYSTEMS

The Dynamic of a River Model Bacterial Community in Two Different Media Reveals a Divergent Succession and an Enhanced Growth of Most Strains Compared to Monocultures

Lise Goetghebuer[1] · Mathias Bonal[1] · Karoline Faust[2] · Pierre Servais[1] · Isabelle F. George[1]

Received: 13 October 2018 / Accepted: 9 January 2019

Abstract

The dynamic of a community of 20 bacterial strains isolated from river water was followed in R2 broth and in autoclaved river water medium for 27 days in batch experiments. At an early stage of incubation, a fast-growing specialist strain, *Acinetobater* sp., dominated the community in both media. Later on, the community composition in both media diverged but was highly reproducible across replicates. In R2, several strains previously reported to degrade multiple simple carbon sources prevailed. In autoclaved river water, the community was more even and became dominated by several strains growing faster or exclusively in that medium. Those strains have been reported in the literature to degrade complex compounds. Their growth rate in the community was 1.5- to 7-fold greater than that observed in monoculture. Furthermore, those strains developed simultaneously in the community. Together, our results suggest the existence of cooperative interactions within the community incubated in autoclaved river water.

Keywords River · Bacteria · Model community · Growth rate · Interactions

Introduction

Freshwater environments are essential on earth and among them, rivers provide a large number of ecosystem services [1]. As open systems, rivers are particularly exposed to anthropogenic stresses and risks of degradation. When flowing through cities, they receive domestic and industrial wastewaters which bring high loads of organic substances and microorganisms and therefore strongly modify not only the physicochemical properties of the rivers but also their microbial communities [2–4].

Compared to other bacterial communities (in soils, oceans, the human gut, etc.), the river bacterial communities remain largely uncharacterized [5]. However, 16S rRNA surveys published to date show that river bacterioplankton is dominated by the same phyla as lake bacterioplankton, i.e., *Proteobacteria* (mostly the Beta and Gamma subclasses), *Actinobacteria*, *Bacteroidetes*, *Verrucomicrobia, Cyanobacteria*, and *Firmicutes* [6–8]. Their relative abundance fluctuates depending on rivers, so that there is no major lineage showing an equally dominating distribution [9]. Some longitudinal studies of river ecosystems revealed that shifts in the bacterial community composition (BCC) often occur along the river course [10–12]. Recently, such shifts were observed at a very fine level of resolution, i.e., within sequence-discrete bacterial populations [13]. Those spatiotemporal changes in BCC result from two major processes: dispersal (due to regional factors) and species sorting (due to local factors). Dispersal refers to the transport of taxa within the lotic habitat and to the input through tributaries convergences or wastewater discharges. Those inputs can lead to the immigration of novel taxa, which can modify permanently, temporarily (resilience), or not at all (resistance) the BCC [14, 15]. The maintenance of immigrant taxa depends on local conditions and their environmental preferences compared to resident strains, resulting in selection, i.e., species sorting [16, 17]. Temperature, dissolved oxygen, pH, particulate organic carbon (POC), dissolved organic carbon (DOC), grazing, and others are all important local factors driving the BCC [18–20]. Finally, the

Electronic supplementary material The online version of this article (https://doi.org/10.1007/s00248-019-01322-w) contains supplementary material, which is available to authorized users.

✉ Isabelle F. George
igeorge@ulb.ac.be

[1] Ecology of Aquatic Systems, Université libre de Bruxelles, Campus Plaine, CP 221, 1050 Brussels, Belgium

[2] Laboratory of Molecular Bacteriology (Rega Institute), Katholieke Universiteit Leuven, Herestraat 49, 3000 Leuven, Belgium

Published online: 24 January 2019

survival of some strains can also depend on direct interactions with other species making up the community. Bacterial cells can exclude or promote other cells' growth through secretion of enzymes, molecules, and/or the emission of signals resulting in positive or negative interactions [21, 22]. For example, some bacterial taxa present streamlined genomes and are auxotrophic for some essential metabolites; their survival in the community is therefore dependent on their metabolic partners which compensate for their lost metabolic function [23, 24].

In rivers, DOC is the primary substrate supporting bacterial growth and respiration [25] and is therefore a focal point of microbial interactions. In this context, metabolic interactions such as competition, cross-feeding, and syntrophy all inextricably modify the fate of microbes in a community [26, 27].

It is highly likely that microbial interactions play a crucial role in community dynamics and ecosystem functioning [28, 29]. Consequently, the deciphering of interactions in microbial communities has become a major focus in microbial ecology. Models analyzing non-random patterns of taxonomic distribution among multiple samples of microbial communities make the prediction of potential microbial relationships possible [30, 31]. For example, using such tools, Widder et al. suggested the existence of positive and negative interactions occurring between the species composing biofilm communities of more than 114 streams in Austria [32]. However, the experimental validation of those interactions remains scarce.

Mixed cultures can be used as model communities in order to study ecological interactions among microorganisms under controlled and reproducible conditions [23]. In this study, we worked with a model riverine microbial community composed of 20 strains belonging to genera commonly found in rivers, which were mainly isolated from the Zenne River (Belgium). The carbon source utilization profile of each strain and of the 20-strain community was determined in a previous study [33], whose results suggested interspecific interactions occurring in that community. In this study, we further analyzed the dynamic of the 20-strain community in two complex media: R2, a common medium used to isolate and study freshwater bacteria and a medium Z made of autoclaved, filtered river water. Bacterial abundance and community structure were measured over a period of 27 days, and the growth of the 20 strains was compared both in monoculture and in the community to assess the impact of species on each other.

Methods

Community Composition and Carbon Source Utilization Profiles

In a previous study [33], a model river bacterial community composed of 20 strains (Table 1) was built. Sixteen strains were isolated from the water column of the Zenne River (Belgium). This river is located in the Scheldt drainage network and is 103 km long; its watershed (991km^2) is characterized by agricultural activities in its upstream part and by a heavily urbanized area (Brussels area) in its downstream part [34]. The sampling site was located upstream from Brussels (Lembeek, 50°42′34.56"N, 4°13′3.30″E). A total of 94 strains were isolated on two different media: R2A (Melford, Ipswich, UK) and a medium named Z consisting of water from the sampling site filtered on 0.2-μm pore-size membranes (Whatman, Maidstone, UK) and autoclaved (20 min at 121 °C), mixed with 15 g/L of agar (VWR, Radnor, USA). The plates were incubated for up to 15 days at 20 °C, a temperature usually reached in the Zenne River in the summer [4]. Most bacteria were isolated after 4, 8, and 15 days of incubation. Of these 94 strains, 16 were chosen to build up a synthetic river bacterial community based on BCC measured in situ at the same sampling station [4] and/or BCC mentioned in other studies on riverine bacterial community composition [7, 10, 15, 35]. The selected strains belonged to ubiquitous genera representing more than 1% of the community composition in at least one of the aforementioned datasets. In addition, four strains belonging to genera/species frequently detected in river water were purchased from the DSMZ (Braunschweig, Germany) culture collection: *Sphingobacterium psychroaquaticum* 22,418, *Rhodoferax fermentans* 10,138, *Limnohabitans curvus* 21,645, *Polynucleobacter cosmopolitanus* 21,490. The carbon source utilization profile of each individual strain and of the mixed community was measured by Goetghebuer, Servais, and George [33] in Phenotype MicroArrays PM1 and PM2A microplates (Biolog, Hayward, USA) that allowed testing 190 different carbon sources.

Experimental Design

The growth of our model community was followed in batch experiments incubated at 20 °C using two media: R2 broth (Melford, Ipswich, UK) and Z medium. First, each of the 20 strains composing the community was grown in Z medium separately. After 48 h, the cell concentration was measured by flow cytometry (following the flow cytometry protocol described below). Each monoculture was then diluted (in Z medium) to a concentration of 5.0×10^4 cells/mL, and all monocultures were mixed together in equal volume. At time zero of the experiment, a volume of 10 mL of the equi-abundant mix was inoculated in bottles containing 1 L of the medium Z or R2 to reach an initial concentration of 5.0×10^2 cells/mL. For both media, four replicates named a, b, c, d in R2 and e, f, g, h in Z were run in parallel (i.e., 8 bottles in total). A fifth uninoculated replicate in R2 and in Z was monitored as negative control. No contamination was detected during the course of the experiment. The bottles were incubated at 20 °C and

Table 1 Identification of the strains making up the synthetic community, their individual growth rates in R2 and Z media and their growth rate ratio (μ_Z/μ_{R2}). The growth rates of the 20-strain community are given in the last line of the table. *ND* not determined

Growth rate μ (h^{-1})				
Strain number	*Identification*	μ_{R2}	μ_Z	*Ratio* μ_Z/μ_{R2}
28Z	*Arthrobacter* sp.	0.26	0.26	1.00
138R	*Nocardioides* sp.	0.18	0.17	0.94
168R	*Streptomyces* sp.	0.17	ND	ND
58R	*Streptomyces* sp.	ND	ND	ND
515Z	*Flavobacterium* sp.	0.42	0.19	0.45
94R	*Flavobacterium* sp.	0.34	0.23	0.68
18R	*Bacillus* sp.	0.39	0.03	0.08
18Z	*Brevundimonas* sp.	0.47	0.03	0.06
124Z	*Hydrogenophaga* sp.	0.33	0.14	0.42
114R	*Rhizobium* sp.	0.2	0.16	0.8
78R	*Janthinobacterium* sp.	0.95	0.2	0.21
21,645	*Limnohabitans curvus*	0.09	0.09	1
21,490	*Polynucleobacter cosmopolitanus*	0.19	0.07	0.37
10,138	*Rhodoferax fermentans*	0.24	0.15	0.63
1315Z	*Variovorax* sp.	0.38	0.14	0.37
44Z	*Acinetobacter* sp.	0.8	0.26	0.32
148R	*Dechloromonas* sp.	0.14	0.03	0.21
218R	*Sphingobacterium* sp.	0.16	ND	ND
84R	*Flavobacterium* sp.	0.4	0.24	0.6
22,418	*Sphingobacterium psychroaquaticum*	0.27	0.11	0.41
	20-strain community	0.73	0.47	0.64

agitated at 250 rpm for up to 662.5 h, corresponding to 27 days. For the first 72 h, the batch experiments were sampled every hour for flow cytometry measurements, then a longer time period was allowed between samplings. Flow cytometry was used to measure cellular concentrations in each sample in triplicate. Aliquots (25 to 50 mL) of each bottle were collected at 11 sampling times (0 h, 10 h, 19 h, 35.5 h, 47.5 h, 60.5 h, 72.5 h, 186.5 h, 331 h, 519.5 h, 662.5 h) to assess community composition. At the last four sampling times, 50 mL of fresh sterile medium was added to the batch experiment to keep a final volume superior to 500 mL.

Bacterial Enumeration by Flow Cytometry

Samples (300 μL) were fixed with paraformaldehyde (3% final concentration), left for 15 min at 4 °C, and then stored frozen at − 20 °C. Prior to analysis, samples were serially 10-fold diluted in 0.22 μm-filtered phosphate-buffered saline preheated at 37 °C and cell counting was performed on two dilutions to target an ideal rate of 200 to 2000 cells/s. Flow cytometry analysis was performed according to the procedure described in Van Nevel et al. [36] with modifications. Cells were stained with SYBR GREEN I (10,000-fold diluted from stock; Amresco, Solon, USA) in addition to Na_2EDTA (5 mM final concentration) to improve outer membrane permeabilization [37]. This was followed by a 13-min incubation in the dark at 37 °C. Stained samples were inoculated in triplicate in a microplate and analyzed using an Accuri C6 flow cytometer (BD, Franklin Lakes, US), equipped with an autoloader. Bacterial abundance (BA, cells/mL) was calculated by counting fluorescent events in 25 μL after gating plots on green (FL1) vs red (FL3) fluorescence. Growth curves of replicates in both media were built from the mean of the BA calculated in triplicate at each sampling time.

DNA Extraction and Illumina Sequencing

Aliquots (25 to 50 mL) of each bottle were collected and bacterial biomass was concentrated by filtration through a 0.2 μm pore-size, 47 mm diameter polycarbonate filter (Millipore, MA). All filters were stored at − 20 °C until use. Genomic DNA extraction was performed with the DNeasy PowerWater Kit (Qiagen, Hilden, Germany) following the manufacturer's protocol. The concentration and purity of the extracts were estimated using a Nanodrop ND-2000 UV-Vis spectrophotometer (Thermo Fisher Scientific, Waltham, US). The V4 region of the 16SrRNA gene was amplified with primers 515F (GTGCCAGCMGCCGCGGTAA) [38] and 806bR (GGACTACNVGGGTWTCTAAT) [39] (http://www.earthmicrobiome.org/) and sequenced on an Illumina MiSeq at StarSEQ laboratory (Mainz, Germany) following a paired-end approach. Sequences were trimmed at 240 bp and

then used for downstream analysis with the open-source software program MOTHUR (http://www.mothur.org) [40]. Reads were assembled into contigs, and contigs shorter than 275 bp or containing ambiguous bases were removed from our dataset. Remaining contigs were aligned against the silva.nr_v132.align file trimmed to the V4 region, preclustered to decrease the number of uniques, and screened for chimeras using the vsearch program. Remaining sequences (contigs) were classified using a homemade database consisting of the whole 16S rRNA gene sequence of the 20 strains. The latter were obtained by Sanger sequencing following a protocol detailed in Goetghebuer, Servais, and George [33]. Relative abundance of a given taxon was set as the number of sequences affiliated with that taxon divided by the total number of sequences per sample. A correction factor was calculated for each strain based on the difference at time zero between the theoretical relative abundance of that strain (1/20) and the observed relative abundance in the Illumina dataset. This correction factor was further applied to all samples. Finally, absolute abundance of a given taxon was obtained by multiplying its relative abundance with the total BA in the relevant sample.

Growth Rates

To estimate their growth rate, the 20 strains were grown in pure culture in R2 and Z media separately. At mid-exponential growth phase, a volume of each culture was inoculated in 20 mL of R2 and Z media so that the initial concentration was close to 5.0×10^2 cells/mL as in the follow-up of the community growth. Monocultures were incubated at 20 °C and 250 rpm for 72 h. Samples of 300 μL were collected and processed for flow cytometry analysis as explained above. Ln(BA) was plotted versus time; growth rate (μ) was obtained by calculating the slope of the straight line fitting the data in the exponential phase. Individual growth rate of a given taxon in the community was calculated as explained above, after plotting Ln-transformed absolute abundances of that taxon in the community versus time.

Statistical Analysis

Absolute abundances were square-root transformed before calculating a Bray-Curtis similarity matrix. The compositional similarity between samples was visualized by a non-metric multidimensional scaling (NMDS) analysis using PRIMER 7 [41]. NMDS plots represent relative distances among samples in relation to the rank order of their relative similarities. A Pearson correlation test was used to identify the strains best correlated with the Bray-Curtis similarity indexes in the NMDS plot. Similarity percentage (SIMPER) was used to determine which strain contributed most to the dissimilarity between sampling times. For alpha diversity analysis, Pielou's evenness index [42] was calculated for each replicate, and means of the four replicates were compared between media. Finally, for both media, the means of the community composition dissimilarity across replicates at each sampling time (Bray-Curtis dissimilarity) were compared.

Results

Growth Rates

Table 1 displays the growth rates of the strains making up the community. Individual growth rates in monoculture ranged from 0.09 to 0.95 h^{-1} in the R2 medium and from 0.03 to 0.26 h^{-1} in the Z medium. For both media, the lower and the higher growth rates differed by a factor of about 10. In all cases, growth rates in Z were smaller than those in R2 or equal. In both media, the same strain reached the highest maximal bacterial abundance: *Hydrogenophaga* sp. 124Z (data not shown). The ratio of growth rates in both media (μZ/μR2) made it possible to separate strains showing similar growth rates in both media from those with different ones. Some strains had no medium preference: *Nocardioides* sp. 138R, *Arthrobacter* sp. 28Z, *Limnohabitans curvus* 21,645. All other strains grew faster in R2 than in Z. The community growth rate in R2 (0.73 h^{-1}) was greater than the growth rate of individual strains except for two. On the other hand, the community growth rate in Z (0.47 h^{-1}) was much higher than any growth rate of individual strains in monoculture.

Bacterial Abundances

In monocultures, maximal bacterial abundances (cells/mL) ranged from 8.0×10^7 to 5.8×10^9 in R2 and from 5.0×10^4 to 5.5×10^6 in Z (data not shown). The growth curves of the community were rather similar in the four replicates (Fig. 1 and Online Resource 1). In R2, the maximal BA ranging from 1.9×10^9 to 3.1×10^9 cells/mL (mean = 2.6×10^9 cells/mL, $n = 4$) was reached after 162 h and fell within the range observed for individual strains, whereas in Z, a maximal BA ranging from 7.8×10^6 to 1.1×10^7 cells/mL (mean = 9.1×10^6 cells/mL, n = 4) was reached after 233 h and was greater than that observed for individual strains. The BA was maintained for 400 h and then slightly decreased at the end of the experiment. In both media, BA measurements across replicates seemed to converge as the coefficient of variation decreased over time (data not shown).

NMDS

Composition similarity between samples across replicates and time was visualized by an NMDS analysis (Fig. 2). In both plots, the first sampling times (10 h in R2, 10 and 19 h in Z)

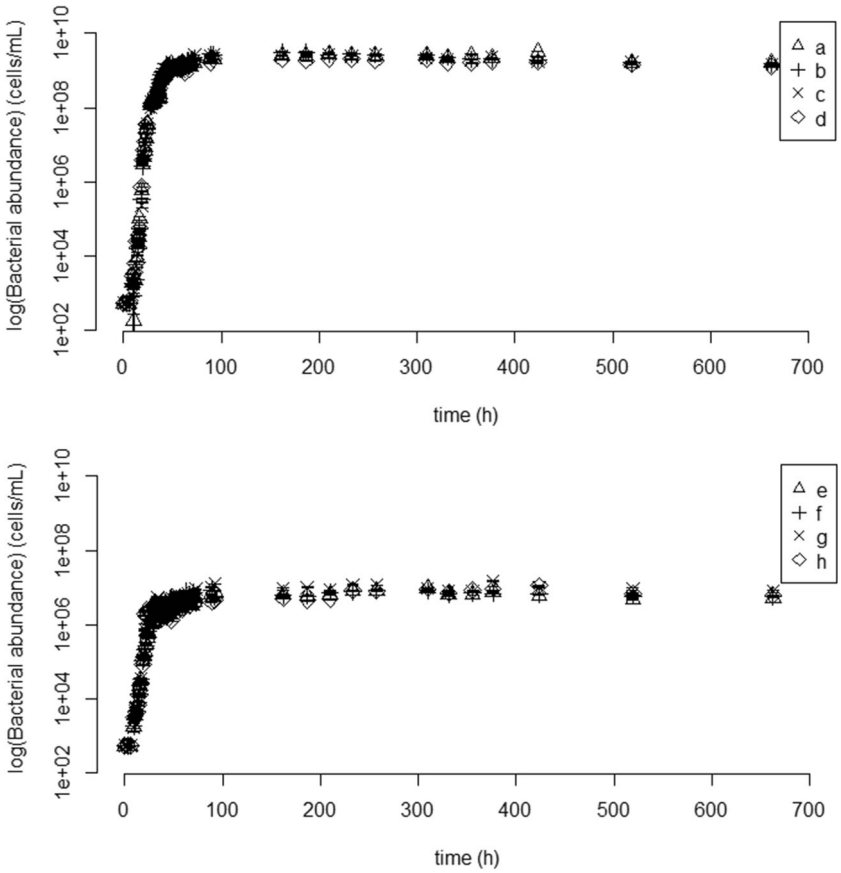

Fig. 1 Logarithm of the bacterial abundance (cells/mL) of the community in the four biological replicates during a 27-day incubation period (20 °C) in R2 medium (left, replicates a–d) and Z medium (right, replicates e–h) measured by flow cytometry. Values are the mean of triplicates and error bars represent standard deviation

were strongly correlated with the absolute abundance of strain 44Z. Three and two temporal clusters could be observed in R2 and Z respectively. In R2, the composition seemed to stabilize after 47.5 h but a third cluster encompassing the last two sampling times appeared to result from the growth of strains 22,418 and 114R (Fig. 2a) whereas in Z, the first four sampling times were quite scattered, the community composition began to stabilize from 60.5 h until the end of the experiment (Fig. 2b).

Community Composition Across Time and Replicates

Analysis of community composition over time confirmed that in each medium, the community evolved in a similar way in the four different bottles over 27 days (Fig. 3). Most of the strains grew in absolute abundance (Online Resource 2), although strains 21,490, 168R and 21,645 in R2, and 21,490 in Z disappeared rapidly. In both media, the relative abundance of strain 44Z (*Acinetobacter* sp) strongly increased since the first sampling time and stayed dominant in the community until 35.5 h in R2 and 47.5 h in Z. After 47.5 h of incubation in R2, the strains with the greatest relative abundance in the community corresponded to strains with a high growth rate in monoculture (i.e., 78R, 44Z, 18R, 515Z, 84R). This matching was not observed in the Z medium.

Over the entire course of the experiment, the strains whose relative abundance rose transiently (and then declined) or progressively (up to the end of the experiment) in R2 were 515Z, 18R, 114R, 78R, 44Z, 10,138, 148R, 218R, 84R, and 22,418 (Fig. 3a). In Z, they were strains 515Z, 18Z, 124Z, 114R, 78R, 44Z, 1315Z, 148R, 218R, 84R, and 22,418 (Fig. 3b). The growth rate of those strains in the community was then calculated based on their individual absolute abundance in the community, and it was compared to their growth rate in monoculture (Fig. 4). Interestingly, many of those strains displayed a growth rate that was greater in the community than in monoculture in R2, and all of them did in Z. In the latter, growth rates in community were 1 to 7.3-fold greater in community than in monoculture, whereas this multiplying factor did not exceed 2 in R2. Finally, the progressive growth of many strains was concomitant in Z (e.g., 18Z, 124Z, 114R, 1315Z, 148R and 84R). Among these, strains 18Z, 124Z, 114R, and 1315Z grew faster—or exclusively—in the community in Z than in the community in R2.

Alpha and Beta Diversity

The Pielou's evenness index (Fig. 5) and the mean of the Bray-Curtis dissimilarity between replicates (Fig. 6) were calculated over time. For both media, Pielou's index began at 1 as the initial

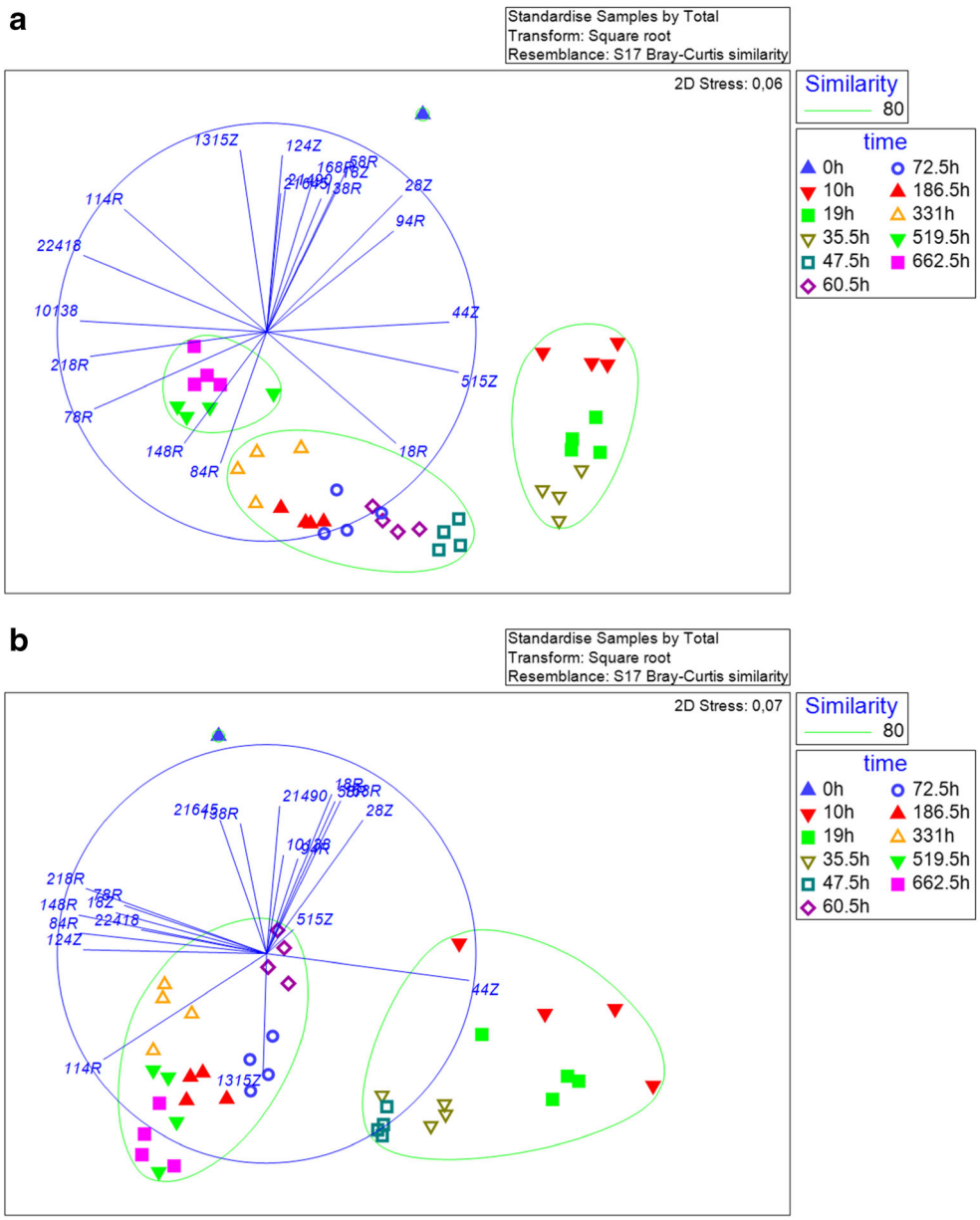

Fig. 2 Non-metric multidimensional scaling plot of the compositional dissimilarities between replicates over time (Bray-Curtis dissimilarities) in R2 (**a**) and Z (**b**) media. The absolute abundance of taxa is plotted as correlation with the samples. The overlaid contours are based on results from group-average cluster analysis (similarity threshold set at 80)

community was equi-abundant (Fig. 5). Then, its value dropped sharply for the first two sampling times, and finally increased until it reached a plateau which was higher in Z than R2.

The mean of community composition's dissimilarity (Bray-Curtis) across replicates slightly decreased over time only in R2 (Fig. 6), but in both cases, the variability between replicates decreased. In other words, for both media, community composition converged across the different replicates.

Discussion

The individual growth rates of our strains in monoculture in Z medium (Table 1) were mostly consistent with rates measured on major bacterioplankton groups in freshwater habitats in the same range of temperature [43]. The 10-fold difference in individual growth rates between the slowest and the fastest-growing strains is not surprising, as previous studies reported that in situ growth rates vary greatly within and between the major phylogenetic groups of bacteria found in aquatic systems [44, 45]. In addition, the ability of some strains to grow fast in monoculture allowed them to dominate the community at the beginning of the experiment in the R2 community, but not necessarily later on. As expected, most strains grew faster in R2 than in Z. But some strains were growing similarly in both media, which means that the amount of substrate assimilable by those strains in Z was large enough to sustain maximal growth rate at 20 °C.

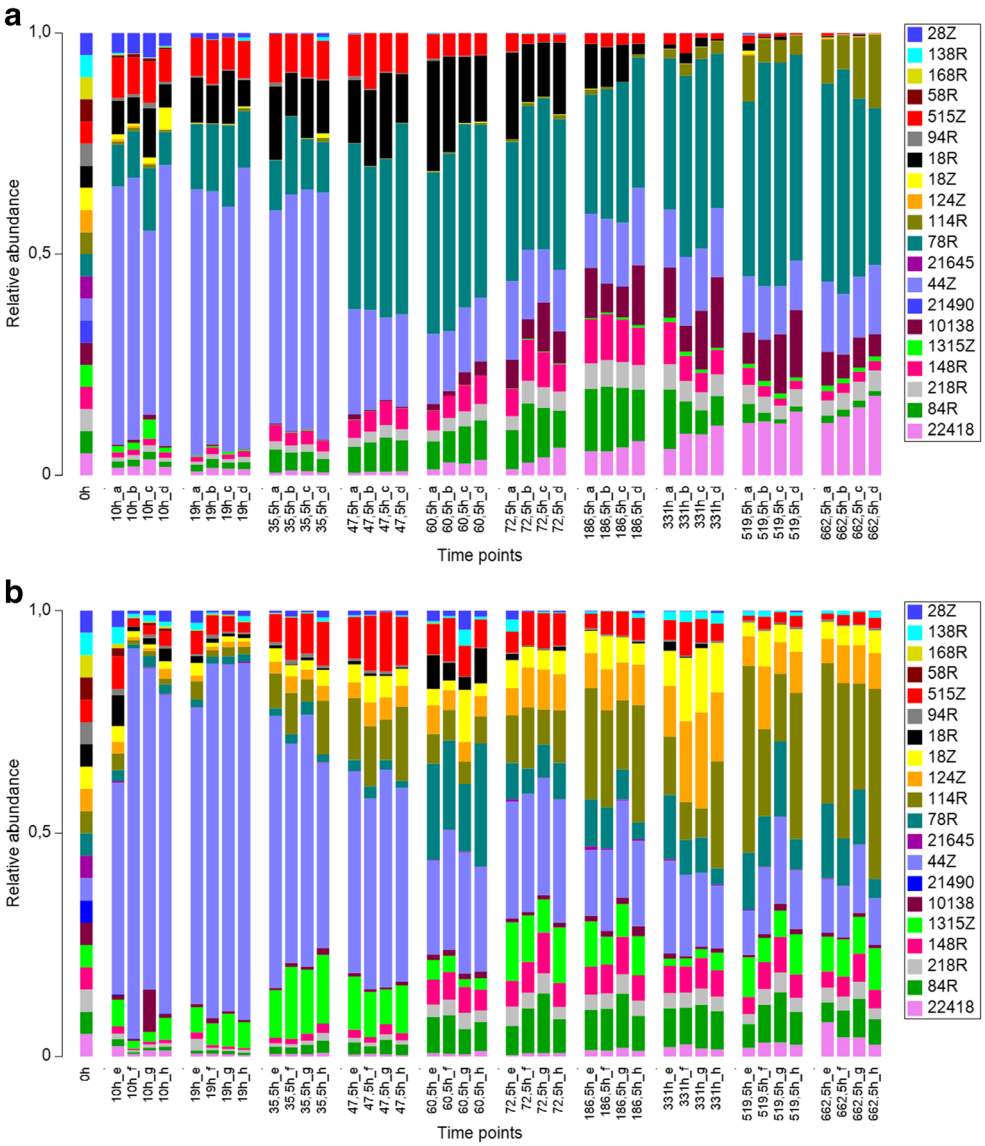

Fig. 3 Relative abundance of the 20 bacterial strains forming the community at the different sampling times in R2 medium (**a**) and Z medium (**b**). For each time point, there are four replicates (a–d in R2 and e–h in Z). Colors refer to strain numbers indicated in Table 1

When the 20 strains were grown in community in R2 (Fig. 1), the average community growth rate measured (0.73 h^{-1}) was consistent with previous maximal growth rates (at saturating carbon concentrations) measured at 20 °C on a natural riverine community [46]. On the contrary, the community growth rate measured in Z (0.47 h^{-1}) was much higher than previous observations of in situ growth rates of riverine bacterial communities (estimated as the ratio between bacterial production and biomass) at the same temperature [45, 47]. This could be due to greater carbon availability in the Zenne River water than in other rivers [34]. Indeed, DOC values in the sampling station of the Zenne River fluctuate between 6 and 8 mgC/L over a year [4]. The latter values are slightly greater than the median DOC values in rivers worldwide (5 mgC/L) as mentioned in the review by Meybeck [48]. Comparison of the mean maximal abundances in R2 and in Z revealed a factor 284 between those values. This can be explained by the amount of biodegradable organic carbon available. Indeed, dissolved organic matter in both media was estimated through the chemical oxygen demand (COD) test according to standard procedure (HACH, Loveland, CO). The COD in R2 and Z were respectively 2710 and 16 mg O_2/L, which correspond to a DOC value of 1016 and 6 mg C/L (assuming that 1 mol of oxygen is necessary to biodegrade 1 mol of carbon). The ratio (COD_{R2}/COD_Z) was thus 169. If we consider that all the dissolved organic carbon is biodegradable in R2 and around 50% of it in the Zenne River water (Servais, unpublished results), the ratio of the biodegradable organic carbon between both media is about 338. This latter ratio is in the same range as the maximal community BA ratio (284) confirming that maximal bacterial abundances reached in these batch experiments were controlled by the biodegradable organic carbon, as usually observed for heterotrophic aquatic bacteria [49].

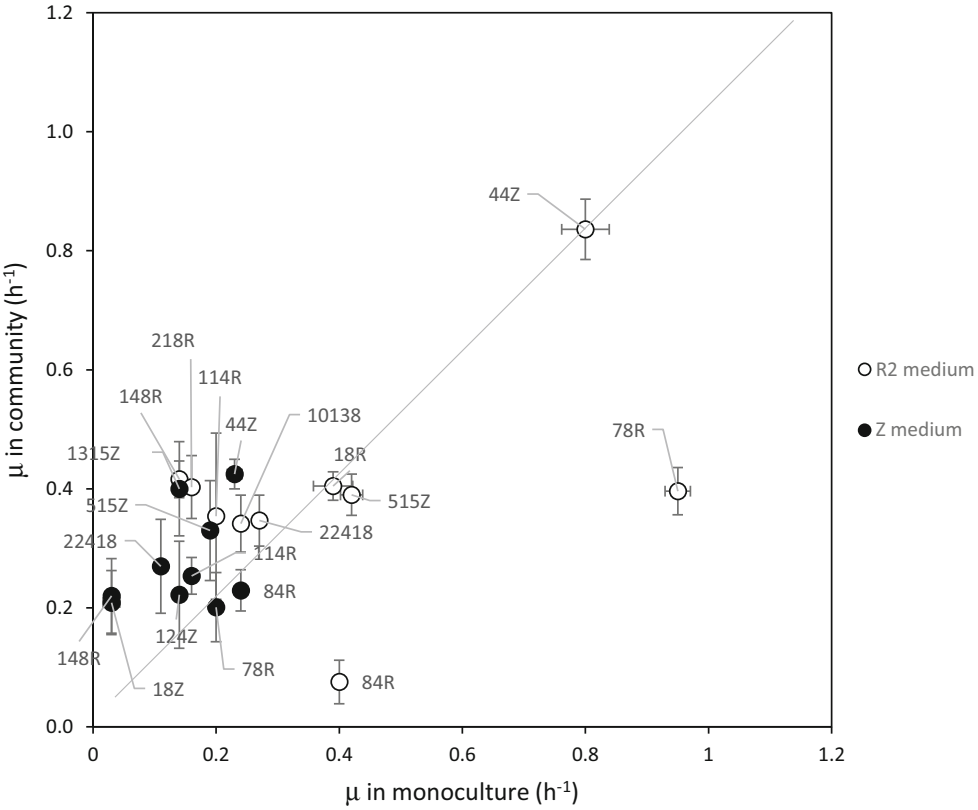

Fig. 4 Growth rate of strains showing transient or progressive growth in the community (h^{-1}) on Fig. 3 as a function of their growth rate measured in monoculture (h^{-1}) in R2 medium (open circles) and Z medium (full circles). The diagonal represents an identical growth rate in community and monoculture. The data point representing 218R in Z medium is missing because its growth rate in monoculture was not measured (see Table 1). Error bars are displayed on the graph ($n = 3$ and 4 for μ in monoculture and in community, respectively)

Although the batch experiments began with an initial abundance identical for each taxon (time 0 in Fig. 3), their community composition shifted several times in both media leading to different clusters in the NMDS plots (Fig. 2). In both media, the early dominance of strain 44Z (*Acinetobacter* sp), a γ-proteobacterium, is probably explained by its high growth rate: 0.8 and 0.26 h^{-1} in R2 and Z, respectively. When looking at its carbon utilization profile, this strain could be classified as a specialist, since it efficiently catabolized a small number of the carbon sources tested in PM microplates [33]. The strain *Acinetobacter* sp. likely stopped increasing concomitantly with a depletion of such carbon sources (see absolute abundance in Online Resource 2). In parallel, an increase of strains all displaying more complex carbon utilization profile (in terms of the number of carbon sources catabolized in PM microplates) could be observed. All those shifts occurred at the same time within the replicate bottles. In both media, community composition showed great convergence among replicates over the entire experiment (Fig. 6), which means that the factors driving it were stable and reproducible.

The individuals composing the community were all heterotrophic strains originating from a river water environment. The quantity and quality of organic matter have been shown to impact abundance, diversity, and activity of heterotrophic microbial communities [49–51]. In that respect, our media displayed strong carbon supply differences. The R2 medium

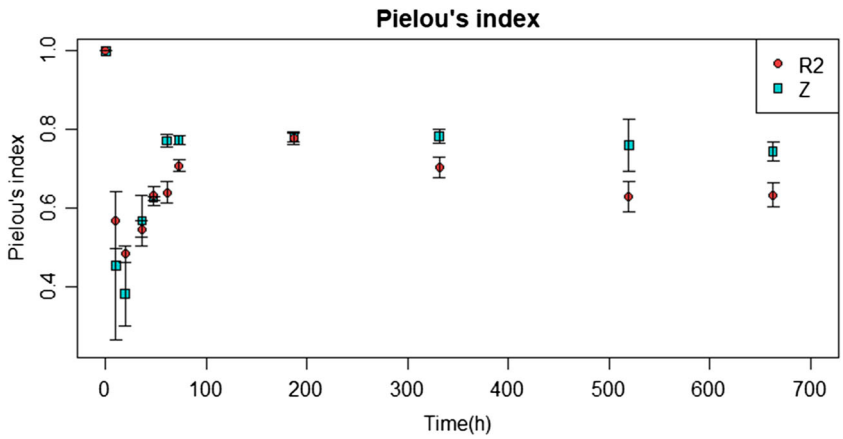

Fig. 5 Temporal development of Pielou's evenness index in R2 and Z media. A mean index was calculated based on the four replicates and is plotted the graph

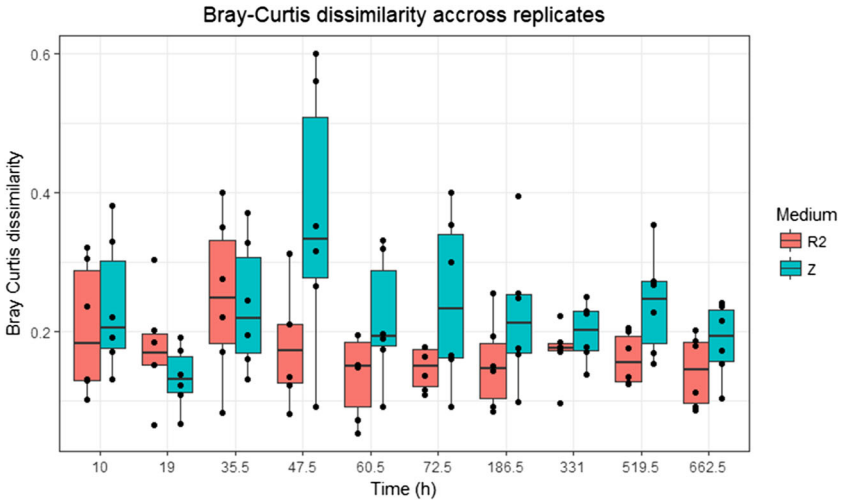

Fig. 6 Mean of the community composition dissimilarity across replicates for each time point (Bray-Curtis dissimilarity) for R2 (pink) and Z (blue) media

contains a high concentration of dissolved organic carbon (DOC) including mainly easily biodegradable compounds such as dextrose, peptone, and yeast extract. The four strains growing faster in R2 than Z, 18R (*Bacillus* sp), 78R (*Janthinobacterium* sp), 22,418 (*Sphingomonas psychroaquaticum*), and 10,138 (*Rhodoferax fermentans*), strongly degraded almost all simple carbon sources (monosaccharides, disaccharides) tested in the PM plates in Goetghebuer, Servais, and George [33]. The ability of strains 22,418 and 10,138 to use simple carbon sources was previously reported [52, 53]. Those strains were therefore probably more competitive regarding easily biodegradable organic carbon compounds than the other strains.

On the other hand, river water DOC is usually composed of a complex mixture of organic compounds differing in their bioavailability: from labile DOC (easily degraded by microbes) to recalcitrant DOC (refractory to degradation) [25]. We assume that during the experiment, the more labile DOC was preferentially consumed, and therefore the less biodegradable part increased relatively. This probably explains why the strains 114R (*Rhizobium* sp.), 124Z (*Hydrogenophaga* sp.), 18Z (*Brevundimonas* sp.), and 1315Z (*Variovorax* sp.), which all grew faster or exclusively in the community incubated in Z compared to that incubated in R2 medium, also belonged to genera reported for their ability to degrade phenolic compounds [54–57]. Another study even mentioned a *Variovorax* sp. as part of a cooperative pesticide-degrading consortium [58]. Recently, Rivett et al. [59] observed in batch experiments that changes in resource utilization (from labile to more recalcitrant substrates) were associated with a shift in microbial interactions from strongly negative interactions to a more neutral state.

In our case, the surprisingly high growth rate and final BA achieved by the community in the Z medium as well as the identity of the dominant strains in that community are all strong arguments suggesting that cooperative interactions occurred. The assumption of positive intracommunity relationships is strengthened by the fact that the calculated growth rate of individual strains in the community was often greater than the one measured in monoculture (Fig. 4). Although this was true for many strains in both media, the increase in strain growth rate in the community compared to monocultures was particularly spectacular in Z, including for the four strains which grew faster (or exclusively) and simultaneously in that medium: 114R, 124Z, 18Z, and 1315Z (1.6 to 7-fold increase). Such an enhanced growth was likely caused by an interdependency between some (or all) of those strains. Finally, the greater community evenness observed in Z (Fig. 5) also supports the assumption of cooperative interactions in that community. We have not identified the nature of those interactions yet, but evidence was found in a recent study that within guilds of highly related species competing for a supplied carbon source, dense networks of cross-feeding interactions develop, which may stabilize competition and favor coexistence [60].

The DOC quality and quantity is known to be a driver of the structure of communities. Here, our results suggest that competitive and/or cooperative interactions occurred depending on the quantity (and probably quality) of this DOC. Species sorting in the river water medium selected several dominant strains among which four are potentially cooperative strains degrading complex compounds. Our future work will focus on the dynamics of those strains as a potential consortium.

Acknowledgments The authors thank Adriana Anzil for her contribution to the experimental work. They also thank the reviewers for their careful reading of the manuscript and their constructive comments to improve it.

Funding information This work was supported by the Fonds National de la Recherche Scientifique FRS-FNRS in the scope of the project "DYNAMO" [T.1037.14].

References

1. Sarukhan J, Whyte A, Hassan R, et al (2005) Millenium Ecosystem Assessment: Ecosystems and human well-being. Island Press
2. Drury B, Rosi-Marshall E, Kelly JJ (2013) Wastewater treatment effluent reduces the abundance and diversity of benthic bacterial communities in urban and suburban Rivers. Appl. Environ. Microbiol. 79:1897–1905. https://doi.org/10.1128/AEM.03527-12
3. Gao Y, Wang C, Zhang W, di P, Yi N, Chen C (2017) Vertical and horizontal assemblage patterns of bacterial communities in a eutrophic river receiving domestic wastewater in Southeast China. Environ. Pollut. 230:469–478. https://doi.org/10.1016/j.envpol.2017.06.081
4. García-Armisen T, İnceoğlu Ö, Ouattara NK, Anzil A, Verbanck MA, Brion N, Servais P (2014) Seasonal variations and resilience of bacterial communities in a sewage polluted urban river. PLoS One 9:e92579. https://doi.org/10.1371/journal.pone.0092579
5. de Oliveira LFV, Margis R (2015) The source of the river as a nursery for microbial diversity. PLoS One 10:e0120608. https://doi.org/10.1371/journal.pone.0120608
6. Kaevska M, Videnska P, Sedlar K, Slana I (2016) Seasonal changes in microbial community composition in river water studied using 454-pyrosequencing. SpringerPlus 5(409):409. https://doi.org/10.1186/s40064-016-2043-6
7. Kolmakova OV, Gladyshev MI, Rozanov AS, Peltek SE, Trusova MY (2014) Spatial biodiversity of bacteria along the largest Arctic river determined by next-generation sequencing. FEMS Microbiol. Ecol. 89:442–450. https://doi.org/10.1111/1574-6941.12355
8. Niño-García JP, Ruiz-González C, del GPA (2016) Interactions between hydrology and water chemistry shape bacterioplankton biogeography across boreal freshwater networks. ISME J 10:1755–1766. https://doi.org/10.1038/ismej.2015.226
9. Logue JB, Lindström ES (2008) Biogeography of Bacterioplankton in inland waters. Fr. Rev. 1:99–114. https://doi.org/10.1608/FRJ-1.1.9
10. Read DS, Gweon HS, Bowes MJ, Newbold LK, Field D, Bailey MJ, Griffiths RI (2014) Catchment-scale biogeography of riverine bacterioplankton. ISME J 9:516–526. https://doi.org/10.1038/ismej.2014.166
11. Savio D, Sinclair L, Ijaz UZ, Parajka J, Reischer GH, Stadler P, Blaschke AP, Blöschl G, Mach RL, Kirschner AKT, Farnleitner AH, Eiler A (2015) Bacterial diversity along a 2 600 km river continuum. Environ. Microbiol. 17(12):4994–5007. https://doi.org/10.1111/1462-2920.12886
12. Staley C, Unno T, Gould TJ, Jarvis B, Phillips J, Cotner JB, Sadowsky MJ (2013) Application of Illumina next-generation sequencing to characterize the bacterial community of the upper Mississippi River. J. Appl. Microbiol. 115:1147–1158. https://doi.org/10.1111/jam.12323
13. Meziti A, Tsementzi D, Rodriguez-R LM, Hatt JK, Karayanni H, Kormas KA, Konstantinidis KT (2018) Quantifying the changes in genetic diversity within sequence-discrete bacterial populations across a spatial and temporal riverine gradient. ISME J 1. https://doi.org/10.1038/s41396-018-0307-6
14. Allison SD, Martiny JBH (2008) Resistance, resilience, and redundancy in microbial communities. Proc. Natl. Acad. Sci. U. S. A. 105:11512–11519. https://doi.org/10.1073/pnas.0801925105
15. Schultz GE, Kovatch JJ, Anneken EM (2013) Bacterial diversity in a large, temperate, heavily modified river, as determined by pyrosequencing. Aquat. Microb. Ecol. 70:169–179. https://doi.org/10.3354/ame01646
16. Lindström ES, Langenheder S (2012) Local and regional factors influencing bacterial community assembly. Environ. Microbiol. Rep. 4:1–9. https://doi.org/10.1111/j.1758-2229.2011.00257.x
17. Székely AJ, Berga M, Langenheder S (2013) Mechanisms determining the fate of dispersed bacterial communities in new environments. ISME J 7:61–71. https://doi.org/10.1038/ismej.2012.80
18. Portillo MC, Anderson SP, Fierer N (2012) Temporal variability in the diversity and composition of stream bacterioplankton communities. Environ. Microbiol. 14:2417–2428. https://doi.org/10.1111/j.1462-2920.2012.02785.x
19. Xia N, Xia X, Liu T, Hu L, Zhu B, Zhang X, Dong J (2014) Characteristics of bacterial community in the water and surface sediment of the Yellow River, China, the largest turbid river in the world. J. Soils Sediments 14:1894–1904. https://doi.org/10.1007/s11368-014-0974-5
20. Zeglin LH (2015) Stream microbial diversity in response to environmental changes: review and synthesis of existing research. Aquat Microbiol 6:454–469. https://doi.org/10.3389/fmicb.2015.00454
21. Foster KR, Bell T (2012) Competition, not cooperation, dominates interactions among culturable microbial species. Curr Biol CB 22:1845–1850. https://doi.org/10.1016/j.cub.2012.08.005
22. Little AEF, Robinson CJ, Peterson SB, Raffa KF, Handelsman J (2008) Rules of engagement: interspecies interactions that regulate microbial communities. Annu. Rev. Microbiol. 62:375–401. https://doi.org/10.1146/annurev.micro.030608.101423
23. Garcia SL (2016) Mixed cultures as model communities: hunting for ubiquitous microorganisms, their partners, and interactions. Aquat. Microb. Ecol. 77:79–85. https://doi.org/10.3354/ame01789
24. Morris JJ, Lenski RE, Zinser ER (2012) The black queen hypothesis: evolution of dependencies through adaptive gene loss. mBio 3:e00036–e00012. https://doi.org/10.1128/mBio.00036-12
25. Benner R (2003) 5—molecular indicators of the bioavailability of dissolved organic matter. In: Findlay SEG, Sinsabaugh RL (eds) Aquatic ecosystems. Academic Press, Burlington, pp 121–137
26. Seth EC, Taga ME (2014) Nutrient cross-feeding in the microbial world. Front. Microbiol. 5:350–356. https://doi.org/10.3389/fmicb.2014.00350
27. Stubbendieck RM, Vargas-Bautista C, Straight PD (2016) Bacterial communities: interactions to scale. Front. Microbiol. 7:1234–1253. https://doi.org/10.3389/fmicb.2016.01234
28. Jousset A, Schmid B, Scheu S, Eisenhauer N (2011) Genotypic richness and dissimilarity opposingly affect ecosystem functioning. Ecol. Lett. 14:537–545. https://doi.org/10.1111/j.1461-0248.2011.01613.x
29. Hug LA, Co R (2018) It takes a village: microbial communities thrive through interactions and metabolic handoffs. mSystems 3:e00152–e00117. https://doi.org/10.1128/mSystems.00152-17
30. Faust K, Raes J (2012) Microbial interactions: from networks to models. Nat Rev Microbiol 10:538–550. https://doi.org/10.1038/nrmicro2832
31. Fisher CK, Mehta P (2014) Identifying keystone species in the human gut microbiome from metagenomic Timeseries using sparse linear regression. PLoS One 9:e102451. https://doi.org/10.1371/journal.pone.0102451
32. Widder S, Besemer K, Singer GA, Ceola S, Bertuzzo E, Quince C, Sloan WT, Rinaldo A, Battin TJ (2014) Fluvial network organization imprints on microbial co-occurrence networks. Proc. Natl. Acad. Sci. 111:12799–12804. https://doi.org/10.1073/pnas.1411723111
33. Goetghebuer L, Servais P, George IF (2017) Carbon utilization profiles of river bacterial strains facing sole carbon sources suggest metabolic interactions. FEMS Microbiol. Lett. 364:1–6. https://doi.org/10.1093/femsle/fnx098
34. Brion N, Verbanck MA, Bauwens W, Elskens M, Chen M, Servais P (2015) Assessing the impacts of wastewater treatment implementation on the water quality of a small urban river over the past 40 years. Environ. Sci. Pollut. Res. 22:12720–12736. https://doi.org/10.1007/s11356-015-4493-8

35. Ghai R, Rodriguez-Valera F, McMahon KD et al (2011) Metagenomics of the water column in the pristine upper course of the Amazon River. PLoS One 6:e23785. https://doi.org/10.1371/journal.pone.0023785
36. Van Nevel S, Buysschaert B, De Roy K et al (2017) Flow cytometry for immediate follow-up of drinking water networks after maintenance. Water Res. 111:66–73. https://doi.org/10.1016/j.watres.2016.12.040
37. De Roy K, Clement L, Thas O et al (2012) Flow cytometry for fast microbial community fingerprinting. Water Res. 46:907–919. https://doi.org/10.1016/j.watres.2011.11.076
38. Caporaso JG, Lauber CL, Walters WA, Berg-Lyons D, Lozupone CA, Turnbaugh PJ, Fierer N, Knight R (2011) Global patterns of 16S rRNA diversity at a depth of millions of sequences per sample. Proc. Natl. Acad. Sci. U. S. A. 108:4516–4522. https://doi.org/10.1073/pnas.1000080107
39. Apprill A, McNally S, Parsons R, Weber L (2015) Minor revision to V4 region SSU rRNA 806R gene primer greatly increases detection of SAR11 bacterioplankton. Aquat. Microb. Ecol. 75:129–137. https://doi.org/10.3354/ame01753
40. Schloss PD, Westcott SL, Ryabin T, Hall JR, Hartmann M, Hollister EB, Lesniewski RA, Oakley BB, Parks DH, Robinson CJ, Sahl JW, Stres B, Thallinger GG, van Horn DJ, Weber CF (2009) Introducing mothur: open-source, platform-independent, community-supported software for describing and comparing microbial communities. Appl Env Microbiol 75:7537–7541. https://doi.org/10.1128/AEM.01541-09
41. Clarke K, Gorley R (2006) PRIMER v7: user manual/tutorial. **PRIMER-E**
42. Pielou EC (1966) The measurement of diversity in different types of biological collections. J. Theor. Biol. 13:131–144. https://doi.org/10.1016/0022-5193(66)90013-0
43. Šimek K, Hornák K, Jezbera J et al (2006) Maximum growth rates and possible life strategies of different bacterioplankton groups in relation to phosphorus availability in a freshwater reservoir. Environ. Microbiol. 8:1613–1624. https://doi.org/10.1111/j.1462-2920.2006.01053.x
44. Cottrell MT, Kirchman DL (2004) Single-cell analysis of bacterial growth, cell size, and community structure in the Delaware estuary. Aquat. Microb. Ecol. 34:139–149. https://doi.org/10.3354/ame034139
45. Yokokawa T, Nagata T, Cottrell MT, Kirchman DL (2004) Growth rate of the major phylogenetic bacterial groups in the Delaware estuary. Limnol. Oceanogr. 49:1620–1629. https://doi.org/10.4319/lo.2004.49.5.1620
46. Billen G, Servais P (1989) Modélisation des processus de dégradation bactérienne de la matière organique en milieu aquatique. In: Bianchi M, Marty D, Bertrand J-C et al (eds) Micro-organismes dans les écosystèmes océaniques. Masson, pp 219–245
47. Billen G, Servais P, Fontigny A (1988) Growth and mortality in bacterial populations dynamics of aquatic environments. Ergeb Limnol 31:173–183
48. Meybeck M (1982) Carbon, nitrogen, and phosphorus transport by world rivers. Am. J. Sci. 282:401–450. https://doi.org/10.2475/ajs.282.4.401
49. Eiler A, Langenheder S, Bertilsson S, Tranvik LJ (2003) Heterotrophic bacterial growth efficiency and community structure at different natural organic carbon concentrations. Appl. Environ. Microbiol. 69:3701–3709. https://doi.org/10.1128/AEM.69.7.3701-3709.2003
50. Kirchman DL, Dittel AI, Findlay SEG, Fischer D (2004) Changes in bacterial activity and community structure in response to dissolved organic matter in the Hudson River, New York. Aquat. Microb. Ecol. 35:243–257. https://doi.org/10.3354/ame035243
51. Langenheder S, Prosser JI (2008) Resource availability influences the diversity of a functional group of heterotrophic soil bacteria. Environ. Microbiol. 10:2245–2256. https://doi.org/10.1111/j.1462-2920.2008.01647.x
52. Hiraishi A, Hoshino Y, Satoh T (1991) Rhodoferax fermentans gen. nov., sp. nov., a phototrophic purple nonsulfur bacterium previously referred to as the "Rhodocyclus gelatinosus-like" group. Arch. Microbiol. 155:330–336. https://doi.org/10.1007/BF00243451
53. Albert RA, Waas NE, Pavlons SC, Pearson JL, Ketelboeter L, Rossello-Mora R, Busse HJ (2013) Sphingobacterium psychroaquaticum sp. nov., a psychrophilic bacterium isolated from Lake Michigan water. Int. J. Syst. Evol. Microbiol. 63:952–958. https://doi.org/10.1099/ijs.0.043844-0
54. Dejonghe W, Berteloot E, Goris J, Boon N, Crul K, Maertens S, Hofte M, de Vos P, Verstraete W, Top EM (2003) Synergistic degradation of Linuron by a bacterial consortium and Isolation of a single linuron-degrading variovorax strain. Appl. Environ. Microbiol. 69:1532–1541. https://doi.org/10.1128/AEM.69.3.1532-1541.2003
55. Lambo AJ, Patel TR (1221) Isolation and characterization of a biphenyl-utilizing psychrotrophic bacterium, Hydrogenophaga taeniospiralis IA3-A, that cometabolize dichlorobiphenyls and polychlorinated biphenyl congeners in Aroclor. J. Basic Microbiol. 46:94–107. https://doi.org/10.1002/jobm.200510006
56. Parales RE, Harwood CS (2002) Bacterial chemotaxis to pollutants and plant-derived aromatic molecules. Curr. Opin. Microbiol. 5:266–273. https://doi.org/10.1016/S1369-5274(02)00320-X
57. Wang Z, Yang Y, Sun W, Xie S, Liu Y (2014) Nonylphenol biodegradation in river sediment and associated shifts in community structures of bacteria and ammonia-oxidizing microorganisms. Ecotoxicol. Environ. Saf. 106:1–5. https://doi.org/10.1016/j.ecoenv.2014.04.019
58. Breugelmans P, Horemans B, Hofkens J, Springael D (2010) Response to mixed substrate feeds of the structure and activity of a linuron-degrading triple-species biofilm. Res. Microbiol. 161:660–666. https://doi.org/10.1016/j.resmic.2010.06.006
59. Rivett DW, Scheuerl T, Culbert CT, Mombrikotb SB, Johnstone E, Barraclough TG, Bell T (2016) Resource-dependent attenuation of species interactions during bacterial succession. ISME J 10(9):2259–2268. https://doi.org/10.1038/ismej.2016.11
60. Goldford JE, Lu N, Bajic D et al (2018) Emergent simplicity in microbial community assembly. Science 361(6401):469–474. https://doi.org/10.1126/science.aat1168